

The Influence of Swirl Angle on the Irreversibilities in Turbulent Diffusion Flames

Dorin Stanciu*, Mircea Marinescu and Alexandru Dobrovicescu
Dept. of Engineering Thermodynamics, Polytechnic University of Bucharest
Splaiul Independentei 313, Bucharest-Romania
sdorin_ro@yahoo.com

Abstract

The objective of this paper is to investigate the volumetric irreversibilities of turbulent swirling diffusion flames. The theoretical background of analysis relies on the local transport exergy equation, which allows the formulation of the well-known Gouy-Stodola theorem at the continuum level. It is already known that, in the case of turbulent flame, the chemical, thermal and mass diffusion irreversibilities represent in order of enumeration the predominant sources of exergy destruction. But these irreversibilities have a more complicated structure than in the laminar flames because the turbulent fluctuations generate new and important irreversibility sources, strongly influencing all the mechanisms mentioned above. Using numerical techniques for flow and multi-species balance equations, this paper tries to emphasize the role of both, swirling number and turbulent intensity field, not only in the burning process intensification but also in the irreversibility creation.

Keywords: Diffusion flames, numerical simulation, exergy destruction, entropy generation.

1. Introduction

In the field of power generation systems, the chemical to thermo-mechanical exergy conversion using the turbulent diffusion hydro-carbonated flames still plays a significant role. The swirling of the oxidizer stream is the most common technique in stabilizing the flame sheet. But the turbulent heat and mass transfer enhancement obtained this way could lead to the irreversibility growth of this exergy conversion process.

There are many ways to measure the irreversibilities of diffusion burning processes, but according to the second law of thermodynamics, only the entropy generation rate can reveal the entire mechanisms of exergy destruction. The entropy generation rate calculus can be performed at a bulk or continuum level. In the case of forced convection processes, both levels of analysis were first formulated by Bejan (1983) and successfully used by other authors like Sciubba (1998).

At the bulk level, the first work that analyzed the irreversibility structure of combustion belongs to Dunbar and Lior (1994). The continuum level of second law analysis was adopted and applied in the case of laminar flames by Arpaci and Selamet (1988), and Datta (2000).

For turbulent non-reacting and reacting flows, the continuum level of entropy generation analysis was extended by Stanciu et al. (2000, 2001, 2006), who observed that the turbulent fluctuations induce in the mean flow field their specific irreversibility mechanisms, having at least the same order of magnitude as the classical ones, generated by the gradients of mean properties. Using the decomposition of the volumetric entropy generation rate in its mean and turbulent parts, Ertesvag and Kolbu (2005) confirmed the major contribution of fluctuating field in the overall flame irreversibility creation. The volumetric rate of entropy production was also used by Iandoli et al. (2005) in order to understand and model the reaction-rate enhancement of turbulent combustion through acoustic waves.

The goal of this paper is to investigate the irreversibility structure of chemical to thermo-mechanical exergy conversion process in turbulent swirling diffusion flames. The basic strategy of turbulence modeling greatly influences the investigation of the volumetric entropy production structure. For this paper, the widely used eddy diffusivity approach for turbulent flow and the eddy dissipation concept for turbulence-chemistry interaction were chosen. This combination allows us to make the distinction between the mean (large-scale) and the turbulent (small-

* Author to whom correspondence should be addressed.

scale) parts of irreversibility and also, among their viscous, thermal, mass diffusion and chemical components.

2 Mathematical model

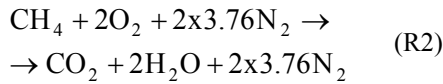
The mathematical model is split into two parts, one referring to the mean flow field and the other to the turbulent reacting flow irreversibilities. This happens because the calculus of the volumetric entropy generation rate needs some basic properties of the fluctuating field resulting from the turbulence closure models.

2.1 Mathematical model of reacting flow

Let us consider a turbulent reacting flow of a gaseous mixture, chemically rouled by the global single step reaction:



where subscripts R and P stand for reactants and products. In this chemical reaction N distinct species are involved. For example, in the case of stoichiometric methane-air combustion:



the chemical species and their stoichiometric coefficients are: $\mathbf{A}_{R,1}=\text{CH}_4$, $\nu_{R,1}=1$, $\mathbf{A}_{R,2}=\text{O}_2$, $\nu_{R,2}=2$, $\mathbf{A}_{R,3}=\text{N}_2$, $\nu_{R,3}=2 \times 3.76$ while $\mathbf{A}_{P,1}=\text{CO}_2$, $\nu_{P,1}=1$, $\mathbf{A}_{P,2}=\text{H}_2\text{O}$, $\nu_{P,2}=2$, $\mathbf{A}_{P,3}=\text{N}_2$ and $\nu_{P,3}=2 \times 3.76$. Obvious in this gaseous mixture is that $N=5$ different species are implicated.

There are many ways to model these flows. For this paper the multi-species approach has been chosen, which is more appropriate to our goals but more expensive from a computational point of view. It is based on the Favre-averaged full Navier-Stokes equations, computed with a turbulence closure and turbulence-chemistry interaction models.

For a steady state reacting flow, the Reynolds-averaged continuity, species, momentum and energy balance equations are (Libby and Williams, 1994):

$$\frac{\partial(\bar{\rho}\tilde{u}_\alpha)}{\partial x_\alpha} = 0 \quad (1)$$

$$\frac{\partial}{\partial x_\alpha} [\bar{\rho}\tilde{u}_\alpha \tilde{Y}_i + \bar{J}_\alpha^{(i)} + \bar{J}_{\alpha,t}^{(i)}] = \beta_M^{(i)} \tilde{\omega} \quad (2)$$

$$\frac{\partial}{\partial x_\alpha} [\bar{\rho}\tilde{u}_\alpha \tilde{u}_\beta + \bar{P}\delta_{\alpha\beta} - \bar{\tau}_{\beta\alpha} - \bar{\tau}_{\beta\alpha,t}] = 0 \quad (3)$$

$$\frac{\partial}{\partial x_\alpha} \left[\bar{\rho}\tilde{u}_\alpha \tilde{h} + \bar{J}_\alpha^{(q)} + \bar{J}_{\alpha,t}^{(q)} + \sum_{i=1}^N \bar{J}_\alpha^{(i)} \tilde{h}_i - (\bar{\tau}_{\beta\alpha} + \bar{\tau}_{\beta\alpha,t}) \tilde{u}_\beta \right] = 0 \quad (4a)$$

where $i=1, N$ identifies the i -species of the gaseous mixture and $\beta_M^{(i)} = -\nu_{R,i} M_{R,i}$ for reactants or $\beta_M^{(i)} = \nu_{P,i} M_{P,i}$ for products. In the total energy balance Equation (4), the kinetic energy, the turbulent kinetic energy and the kinetic energy of diffusion velocity were neglected.

In Equations (1)-(4):

$$\bar{J}_\alpha^{(i)} = -\bar{\rho} D_{im} \frac{\partial \tilde{Y}_i}{\partial x_\alpha} \quad (5a)$$

$$\bar{\tau}_{\beta\alpha} = \mu \left(\frac{\partial \tilde{u}_\alpha}{\partial x_\beta} + \frac{\partial \tilde{u}_\beta}{\partial x_\alpha} - \frac{2}{3} \delta_{\alpha\beta} \frac{\partial \tilde{u}_\gamma}{\partial x_\gamma} \right) \quad (5b)$$

$$\bar{J}_\alpha^{(q)} = -\lambda \frac{\partial \tilde{T}}{\partial x_\alpha} \quad (5c)$$

denote the mass diffusion mean vector, the viscous mean stress tensor and the mean heat flux vector. The energy balance equation can be further simplified. With the supplemental assumption $Le_i=1$, meaning that all species Schmidt numbers are equal to the mixture Prandtl number, Equation (4) takes the form:

$$\frac{\partial}{\partial x_\alpha} \left[\bar{\rho}\tilde{u}_\alpha \tilde{h} - \frac{\lambda}{c_p} \frac{\partial \tilde{h}}{\partial x_\alpha} + \bar{J}_{\alpha,t}^{(q)} \right] = 0 \quad (4b)$$

This assumption is widely used in turbulent combustion models where the turbulent transfer prevails to the mean one and a unique turbulent Schmidt number, Sc_t , is adopted.

The correlations of fluctuating properties appearing in Equations (1)-(4) are expressed by:

$$\begin{aligned} \bar{\tau}_{\alpha\beta,t} &= -\overline{\rho u_\beta'' u_\alpha''} ; \bar{J}_{\alpha,t}^{(q)} = -\overline{\rho u_\alpha'' h''} ; \\ \bar{J}_{\alpha,t}^{(i)} &= -\overline{\rho u_\alpha'' Y_i''} \end{aligned} \quad (6a,b,c)$$

and represent the corresponding Reynolds quantities. In order to solve the system (1)-(5), a closure turbulence model for expression (6) and a combustion model for the mean reaction rate $\tilde{\omega}$ must be added.

Although they have been widely criticized, the second order closure models of turbulent momentum are very practical for engineering calculation. They rely on the Boussinesq approximation which states that:

$$\bar{\tau}_{\alpha\beta,t} = \mu_t \left(\frac{\partial \tilde{u}_\alpha}{\partial x_\beta} + \frac{\partial \tilde{u}_\beta}{\partial x_\alpha} - \frac{2}{3} \delta_{\alpha\beta} \frac{\partial \tilde{u}_\gamma}{\partial x_\gamma} \right) - \frac{2}{3} \delta_{\alpha\beta} \bar{\rho} K \quad (7)$$

where μ_t stands for the turbulent viscosity.

It is well known that the standard K - ε_K model fails in predicting the separated and swirling flows or the spreading rate of round jet, which are most often used in combustion processes. In order to improve its behavior, some corrections on the ε_K equation or some modifications of model constants C_μ , $C_{\varepsilon 1}$ and $C_{\varepsilon 2}$ must be added, but they depend on the flow type. Among all K - ε_K models dealing with these requirements, the RNG formulation seems to be the best choice. For the high Reynolds number regions of the flow, its equations are:

$$\mu_t = \rho C_\mu \frac{K^2}{\varepsilon_K} f\left(\alpha_s, \Omega, \frac{K}{\varepsilon_K}\right) \quad (8)$$

$$\frac{\partial}{\partial x_\alpha} \left[\bar{\rho} \tilde{u}_\alpha K - \alpha_K (\mu + \mu_t) \frac{\partial K}{\partial x_\alpha} \right] = \bar{\tau}_{\beta\alpha,t} \frac{\partial \tilde{u}_\alpha}{\partial x_\beta} - \bar{\rho} \varepsilon \quad (9)$$

$$\begin{aligned} \frac{\partial}{\partial x_\alpha} \left[\bar{\rho} \tilde{u}_\alpha \varepsilon_K - \alpha_\varepsilon (\mu + \mu_t) \frac{\partial \varepsilon_K}{\partial x_\alpha} \right] = \\ = \frac{\varepsilon_K}{K} \left(C_{\varepsilon 1} \bar{\tau}_{\beta\alpha,t} \frac{\partial \tilde{u}_\alpha}{\partial x_\beta} - \bar{\rho} C_{\varepsilon 2}^* \right) \end{aligned} \quad (10)$$

where α_K and α_ε represent the constants of model and $C_{\varepsilon 2}^*$ is computed from an algebraic equation involving the strain rate modulus and the characteristic time of turbulence. Note that in Equation (8) the swirl modification of K - ε_K RNG formulation was used (Fluent Inc., 1998), so that Ω is the characteristic swirl number and α_s is the swirl constant.

Another option for turbulence momentum closure could be the Reynolds stress model (RSM), which employs a balance equation for each individual stress component. The RSMs take into account the anisotropy of the turbulence field, so their results could be better for separating and swirling flows. But the choice of these models enhances the computational effort because, in a 3D case, seven nonlinear PDF equations complete the mean flow system.

Using the similarities between the turbulent transfer of momentum and mass or heat turbulent exchanges, $\bar{J}_{\alpha,t}^{(i)}$ is related to its mean mass fraction gradient through the turbulent mass diffusion coefficient D_t , and $\bar{J}_{\alpha,t}^{(q)}$ is connected to the mean temperature gradient using the turbulent heat transfer coefficient λ_t . These quantities are computed with the aid of turbulent Schmidt and turbulent Prandtl numbers, whose values, $Sc_t=0.7$ and $Pr_t=0.85$, are constant in the entire reacting flow. For the turbulent heat flux, $\bar{J}_{\alpha,t}^{(q)}$, some two equations eddy diffusivity models (Sommer et al., 1997, Deng et al., 2001), or some turbulent heat flux models are available (Seki et al., 2003). Unfortunately, they are made for non-reacting

flows and would not be of any help in improving the numerical solution of the combustion processes. But as will be seen later, they could serve to avoid one of the many approximations of the volumetric irreversibility model. In the case of turbulent mass fluxes, $\bar{J}_{\alpha,t}^{(i)}$, the basic hypothesis $Sc_t=0.7$ remains the only choice.

The turbulence-chemistry interaction models, widely used in the multi-species approach, mix controlled combustion techniques that determine the mean volumetric reaction rate $\tilde{\omega}$ as a function of mean mass fraction field, \tilde{Y}_i and the characteristic time of turbulence. For this work the well-known eddy-break formulation of Magnussen and Hjertager (1976). It sets the volumetric rate of reaction (R1) as:

$$\omega = \min(\tilde{\omega}_1, \tilde{\omega}_2) \quad (11)$$

where:

$$\begin{aligned} \tilde{\omega}_1 &= A \bar{\rho} \frac{\varepsilon_K}{K} \min_i \left(\frac{\tilde{Y}_{R,i}}{v'_R M_{R,i}} \right); \\ \tilde{\omega}_2 &= AB \bar{\rho} \frac{\varepsilon_K}{K} \frac{\sum_j \tilde{Y}_{P,j}}{\sum_j v'_j M_{P,j}} \end{aligned}$$

Indices R and P stand for reactants and products and $A=4.0$ or $B=0.5$ are the model constants.

2.2 Mathematical model irreversibilities

At this time, for the mathematical model of turbulent volumetric irreversibility there are fewer choices, because it is needed to choose from among the multi-species or probability density function approaches (Stanciu et al., 2001) and the eddy diffusivity model of Ertesvag and Kolbu (2005). From the reporting data of the authors the first one, which mathematically is the roughest, closes the bulk entropy balance equation on the flow domain within 7%, the second over predicts the rate of entropy generation with 20% and the third under predicts it with 30%. From the turbulence modeling point of view, the last model is the most promising because it tries to quantify the turbulent irreversibility at the places where it occurs, but it is still under development.

Of course it is impossible to close exactly the entropy equation computing its convection flux at inflow and outflow boundaries with the entropy of the mean flow properties and the overall rate of entropy creation from the volumetric rate of entropy generation integrated on the flow domain. But an error greater than 10% could be unexpected because at inflow and out-

flow boundaries (if the last one is considered far away from the flame sheet), the turbulence intensity is quite a bit lower. Taking into account the fact that we perform a parametric study and we need to close as much as possible the bulk balance of entropy equation, for this study the multi-specie approach was chosen.

At the continuum level, the mathematical model of turbulent multi-component flow irreversibilities relies on the instantaneous expression of the volumetric entropy generation rate (Kondepudi and Prigogine, 1998):

$$\begin{aligned}\sigma^{(s)} &= \sigma_v^{(s)} + \sigma_q^{(s)} + \sigma_d^{(s)} + \sigma_{ch}^{(s)} = \\ &= \frac{\tau_{\beta\alpha}}{T} \frac{\partial u_\beta}{\partial x_\alpha} - \frac{1}{T^2} j_\alpha^{(q)} \frac{\partial T}{\partial x_\alpha} - \\ &\quad - \frac{1}{T} \sum_{i=1}^N j_\alpha^{(i)} \left(\frac{\partial \mu_i}{\partial x_\alpha} \right)_T + \frac{A\omega}{T}\end{aligned}\quad (12)$$

where A represents the chemical affinity. Neglecting all the diffusion phenomena and dropping the serial decompositions of $T^{-2} = \tilde{T}^{-2} (1 + T''/\tilde{T})^{-2}$ and $Y_i^{-1} = \tilde{Y}_i^{-1} (1 + Y_i''/\tilde{Y}_i)^{-1}$ at the first term, the Reynolds-averaged expression of Equation (12) becomes (Stanciu et al., 2001):

$$\begin{aligned}\bar{\sigma}^{(s)} &\cong \bar{\sigma}_{v,m}^{(s)} + \bar{\sigma}_{v,t}^{(s)} + \bar{\sigma}_{q,m}^{(s)} + \bar{\sigma}_{q,t}^{(s)} + \\ &\quad + \bar{\sigma}_{d,m}^{(s)} + \bar{\sigma}_{d,t}^{(s)} + \bar{\sigma}_{ch,t}^{(s)}\end{aligned}\quad (13)$$

Equation (13) reveals that the reacting flow irreversibilities are of two types: either mean, induced by the viscous, thermal and mass diffusion (subscript M), or turbulent induced by the fluctuating components of those fields (subscript T). An exception to this rule is the chemical component, for which only its turbulent part is considered.

The expressions of viscous components are:

$$\bar{\sigma}_{v,m}^{(s)} = \frac{\tilde{\tau}_{\beta\alpha}}{\tilde{T}} \frac{\partial \tilde{u}_\beta}{\partial x_\alpha}\quad (14a)$$

$$\bar{\sigma}_{v,t}^{(s)} = \frac{\bar{\rho} \varepsilon_K}{\tilde{T}}\quad (14b)$$

which model the mean motion irreversibilities due to the gradients of averaged velocity and the mean turbulent irreversibilities, generated by the volumetric dissipation rate:

$$\bar{\rho} \varepsilon_K = \overline{\tau_{\beta\alpha} \left(\frac{\partial u_\beta''}{\partial x_\alpha} \right)}\quad (15)$$

of turbulent kinetic energy, $\bar{\rho} K = \overline{\rho \frac{1}{2} u_\alpha'' u_\alpha''}$.

The mean and turbulent thermal components of volumetric entropy generation rates are expressed by:

$$\bar{\sigma}_{q,m}^{(s)} = \frac{\lambda}{\tilde{T}^2} \frac{\partial \tilde{T}}{\partial x_\alpha} \frac{\partial \tilde{T}}{\partial x_\alpha}\quad (16a)$$

$$\bar{\sigma}_{q,t}^{(s)} = \frac{\bar{\rho} c_p}{\tilde{T}^2} \varepsilon_\theta\quad (16b)$$

where

$$\bar{\rho} \varepsilon_\theta = \overline{\alpha \rho \left(\frac{\partial T}{\partial x_\alpha} \right) \left(\frac{\partial T''}{\partial x_\alpha} \right)}\quad (17)$$

represents the volumetric dissipation rate of fluctuating temperature variance, $K_\theta = \frac{1}{2} \overline{\rho T''^2} / \bar{\rho}$.

The mean and turbulent mass diffusion components of flow irreversibilities are modeled by the following two terms:

$$\bar{\sigma}_{d,m}^{(s)} = \sum_{i=1}^N \bar{\rho} D_{im} \frac{R_i}{\tilde{Y}_i} \frac{\partial \tilde{Y}_i}{\partial x_\alpha} \frac{\partial \tilde{Y}_i}{\partial x_\alpha}\quad (18a)$$

$$\bar{\sigma}_{d,t}^{(s)} = \sum_{i=1}^N \frac{R_i}{\tilde{Y}_i} \bar{\rho} \varepsilon_i\quad (18b)$$

in which:

$$\varepsilon_i = D_{im} \overline{\left(\frac{\partial Y_i''}{\partial x_\alpha} \right) \left(\frac{\partial Y_i}{\partial x_\alpha} \right)}\quad (19)$$

is the volumetric dissipation rate of the fluctuating mass fraction variance $\bar{\rho} K_i = \frac{1}{2} \overline{\rho Y_i''^2}$.

Finally, the turbulent chemical source of the entropy generation rate is approximated by:

$$\bar{\sigma}_{ch,t}^{(s)} \cong \frac{\tilde{\omega}}{\tilde{T}} \left[\sum_i v_{R,i} \tilde{\mu}_{M,i} - \sum_j v_{P,j} \tilde{\mu}_{M,j} \right]\quad (20)$$

where the mean chemical molar potential is simply computed as:

$$\tilde{\mu}_{M,i} = \tilde{h}_{M,i} - \tilde{T}_{S_{M,i}} \left(\tilde{T}, \bar{p}, \tilde{X}_i \right)\quad (21)$$

Clearly here, the mean value of a product is expressed as the product of mean values. It is the roughest approximation appearing in the volumetric irreversibility model. This approximation is imposed by the mathematical model adopted for the turbulent reacting flow which does not offer any information about the other correlations resulting from the modeling of the reaction rate and chemical affinity mean value products.

Let us discuss the implications of the hypothesis in which the volumetric irreversibility model was obtained. The first is serial decomposition. As pointed out by Borghi (1988), the

temperature fluctuations in combustion can be very large. In the case of wrinkled premixed flames, they can exceed the mean temperature of the flow. But for diffusion flames, the temperature variation is more distributed. Therefore, the temperature fluctuations are much smaller and the serial decomposition works. Using this way, two important peculiarities of the irreversibility mechanism of turbulent combustion are emphasized: (1) the entropy creation takes place on both larger and smaller turbulence scales; (2) in all cases, the gas mixture molecular diffusivities are responsible for this creation.

The true problem of this irreversibility model is the dropping of all momentum fluctuations of temperature and species mass fractions, resulting from the serial decomposition. This implication will be discussed in the next section in accordance with the numerical results.

2.3 The gap between models

When the turbulent heat and mass transfer models rely on the classical algebraic relations $Pr_t=const.$ and $Sc_t=const.$, ε_0 and ε_i are unavailable. Therefore, the turbulent thermal and turbulent mass diffusion components of entropy source (13) cannot be computed. In this case, the equilibrium turbulence feature could be invoked. Consequently, the production terms and the dissipation rates of K_0 and K_i are equal so that:

$$\overline{\sigma_{v,t}^{(s)}} \cong \frac{\bar{\rho} c_p \alpha_t}{\bar{T}^2} \frac{\partial \bar{T}}{\partial x_j} \frac{\partial \bar{T}}{\partial x_j} = \frac{\lambda_t}{\bar{T}^2} \frac{\partial \bar{T}}{\partial x_j} \frac{\partial \bar{T}}{\partial x_j} \quad (22)$$

$$\overline{\sigma_{d,t}^{(s)}} \cong \bar{\rho} D_t \sum_{i=1}^N \frac{R_i}{\bar{Y}_i} \frac{\partial \bar{Y}_i}{\partial x_\alpha} \frac{\partial \bar{Y}_i}{\partial x_\alpha} \quad (23)$$

The above equations represent other important approximations of volumetric irreversibility field descriptions, which are obviously induced by the choice of turbulence closure models. Using them in the expression of volumetric entropy generation rates, the turbulent diffusivities of the gas mixture will appear. But it must be emphasized that they are responsible only for the production of the temperature and species mass fraction fluctuations which occur at the larger turbulence scale. Their dissipations, which create the irreversibility, occur at the smaller turbulence scales (Taylor micro-scales). Thus, with the above approximations, we try to quantify at the larger turbulence scales the irreversibility that will occur at the smaller ones. Of course, the existence of a two-equation eddy diffusivity model for turbulent heat and mass fluxes could remove these approximations. Unfortunately at this moment such models exist only for the turbulent heat fluxes, and they are not especially designed for the combustion processes.

The hypothesis $Le=1$ does not affect the accuracy of the bulk closure entropy equation because it was also used for deriving the instantaneous volumetric rate of entropy expression (12). As long as a transfer process is neglected in the energy equation, its corresponding irreversibility must also be neglected in the entropy source.

2.4 Closing the bulk entropy equation

In order to obtain some information about the accuracy of numerical simulation and the verification of the irreversibility model, the closing error of entropy balance on the entire reacting flow domain can be verified. Taking into account that the combustion is adiabatic and neglecting the diffusion fluxes at inflow and outflow boundaries, this equation takes the form:

$$\dot{S}_\Sigma = \sum_j \left(\dot{\bar{S}}_{gen} \right)_j \quad (24)$$

where the convection flux of entropy on the boundaries ∂V is computed as:

$$\dot{S}_\Sigma \cong \int_{\partial V} \bar{\rho} s(\bar{T}, \bar{p}) \vec{u} \cdot \vec{n} d\Sigma \quad (25)$$

and the overall entropy generation rate components are determined by integrating their volumetric rate on the entire flow domain:

$$\left(\dot{\bar{S}}_{gen} \right)_j = \int_V \sigma_j^{(s)} dV \quad (26)$$

In the above expression $j="v,m"$, " v,t ", " q,m ", " q,t ", " d,m ", " d,t ", " ch,t ". As pointed out above, Equation (24) cannot be exactly closed because the entropy convection flux (25) is computed with the entropy of the mean temperature and pressure, $s(\bar{T}, \bar{p})$ and not with the mean entropy of the instantaneous temperature and pressure, $\tilde{s}(T, p)$.

2.5 Exergy balance equation

It is well known that the exergy loss analysis of a thermodynamic process can be based either on the exergy balance equation or, according to the Gouy-Stodola theorem, on the entropy source. In this latter case, the continuum level of second law analysis is suitable because it takes into account the local non-equilibrium of exergy transfer processes. Following this idea, it could be useful to obtain at a continuum level (even in an approximate manner) the balance equation of mean thermo-mechanical exergy, because it can help us understand how the volumetric irreversibility component acts and destroys the exergy during mass heat and diffusion transfer processes.

The instantaneous form of this equation is obtained by combining the balance equations of total energy and entropy, the last one multiplied with the reference temperature $T_0=298.15$ K, at which the formation state of all mixture components is defined. Then, after some algebraic transformations and some classical approximations of Favre averaging technique it reads:

$$\frac{\partial}{\partial x_\alpha} \left[\bar{\rho} \tilde{u}_\alpha (\tilde{e}_{th}) + \bar{E}_{\alpha,eff}^{(i)} + \bar{E}_{\alpha,eff}^{(q)} + \bar{E}_{\alpha,eff}^{(\tau)} \right] + \frac{\partial \bar{\Phi}'}{\partial x_\alpha} + \sum_{i=1}^N \bar{j}_\alpha^{(i)} \frac{\partial \bar{\mu}_{i,0r}}{\partial x_\alpha} = \bar{\Pi}(\tilde{e}_{th}) - \bar{\Delta}(\tilde{e}_{th}) \quad (27)$$

Equation (27) is written in the general form of a scalar conservation law. It shows that at continuum level, the transfer of thermo-mechanical exergy is due to its mean convection flux, $\bar{\rho} \tilde{u}_\alpha \tilde{e}_{th}$ and to its mean diffusion fluxes, due to the heat, mass and work interactions. They can be expressed as:

$$\bar{E}_{\alpha,eff}^{(i)} = \bar{E}_\alpha^{(i)} + \bar{E}_{\alpha,t}^{(i)} = \bar{j}_\alpha^{(i)} e_{th}^{(i)} + \bar{j}_{\alpha,t}^{(i)} \tilde{e}_{th}^{(i)} \quad (28)$$

$$\bar{E}_{\alpha,eff}^{(q)} = \bar{E}_\alpha^{(q)} + \bar{E}_{\alpha,t}^{(q)} = \bar{j}_\alpha^{(q)} (1 - T_0/T) + \bar{j}_{\alpha,t}^{(q)} (1 - T_0/\tilde{T}) \quad (29)$$

$$\bar{E}_{\alpha,eff}^{(\tau)} = \bar{E}_\alpha^{(\tau)} + \bar{E}_{\alpha,t}^{(\tau)} = -(\bar{\tau}_{\beta\alpha} + \bar{\tau}_{\beta\alpha,t}) \tilde{u}_\beta \quad (30)$$

where $\tilde{e}_{th}^{(i)} = \tilde{h}_i - h_{i,0r} - T_0(\tilde{s}_i - s_{i,0r})$ is the mean thermo-mechanical specific exergy convected by the relative velocity of the i^{th} -component in the mixture. The subscript $0r$ denotes the restricted dead state, defined by the reference T_0 and P_0 of the environment and by the molar fractions, X_i or mass fractions Y_i existing in each flow point. Clearly here, because of the chemical composition variations, the restricted dead state differs from one flow point to another one.

Each component defined by the Equations (28)-(30) is separated into two parts, the first one generated by the mean gradients and the other by the turbulent fluctuations of flow properties. At the continuum level, the relative importance of each exergy transfer mechanism depends on flow geometry, flow initial conditions and the spatial location of every analyzed region. But in all cases, the turbulent exergy component of each mechanism will overcome the mean one because the turbulent part of energy fluxes also prevails.

The last term appearing on the left-hand side of Equation (27) takes into account the change of thermo-mechanical exergy due to the spatial modification of the restricted dead state through the mass or molar fraction variation.

The volumetric source appearing in the above equation contains both the production and destruction (dissipation) terms. The mean volu-

metric rate of thermo-mechanical exergy production:

$$\bar{\Pi}(\tilde{e}_{th}) = \bar{\zeta}_{ch} \bar{\omega} \quad (31)$$

is proportional to the fraction of chemical fuel exergy:

$$\zeta_{ch} = - \left\{ \Delta G^{(o)} + R_M \tilde{T}_0 \ln \left[\prod_j x_j^{v_{P,j}} / \prod_i x_i^{v_{R,i}} \right] \right\} \quad (32)$$

which is locally released with a velocity equal to the chemical reaction rate, ω . In the above relation:

$$\Delta G^{(o)} = \sum_j v_{P,j} g_{M,P,j}^{(o)} - \sum_i v_{R,i} g_{M,R,i}^{(o)} \quad (33)$$

is the change of Gibbs free energy of formation over the chemical reaction (R1), and $g_{M,k}^{(o)}$ represents the molar specific Gibbs function of the k^{th} specie, evaluated at reference standard state defined by $T_0=298.15$ K and $P_0=1.013$ bar. It must be emphasized that not all chemical fuel exergy is transferred to the thermo-mechanical part. In every point of reacting flow, the available chemical exergy of the fuel is $\bar{Y}_{fu} e_{ch}^{(fu)}$, where $e_{ch}^{(fu)}$ is computed with the classical relation of Moran and Shapiro (2006). While $\bar{\zeta}_{ch}$ is transferred to the thermo-mechanical field, the difference $\bar{Y}_{fu} e_{ch}^{(fu)} - \bar{\zeta}_{ch}$ is used to balance the chemical exergy gap between the oxidant and the combustion products.

More important for our goal is the volumetric rate of exergy destruction:

$$\bar{\Delta}(\tilde{e}_{th}) = T_0 \bar{\sigma}^{(s)} > 0 \quad (34)$$

Of course the relation (34) represents the local formulation of the Gouy-Stodola theorem.

Resulting from Equation (27) the exchange of the mean thermo-mechanical exergy is due to the mean and turbulent diffusion transfer of heat, mass and momentum. But as revealed by Equations (28)-(30), each diffusion form of exergy exchange is accompanied by its peculiar mechanism of entropy generation (exergy destruction). Note that the mean components model the irreversibility created at the largest scales of turbulence, while the turbulent ones characterize the irreversibility generated by the smallest turbulence scales.

The process of chemical to thermo-mechanical exergy conversion is also accompanied by irreversibility generation. In this case, the mixing of fuel and oxidizer is controlled by the turbulent mass transfer between the large and

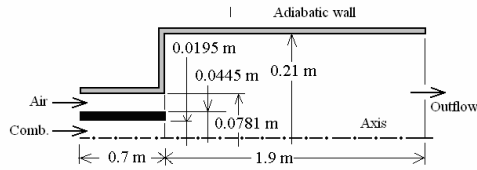
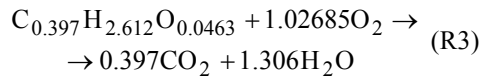


Figure 1. The geometry of numerical simulation

the fine turbulence structures. As a result, only the turbulent volumetric part of the chemical entropy generation rate was retained.

Results and discussions

For the numerical analysis the axisymmetric geometry presented in Figure 1 (Lockwood et al., 1974) was chosen. The original gas fuel had the following volumetric composition: 27% CH₄, 55% H₂, 4% CO, 2% C₂H₆, 8% CO₂ and 4% N₂; but in order to reduce the number of solved equations, this fuel was replaced with an equivalent gas mixture having the mass fraction composition of 0.6068 for C_{0.397}H_{2.612}O_{0.0463}, 0.298 for CO₂ and 0.0952 for N₂. Then, the resulting stoichiometric chemical reaction was:



At the end of the coflowing air stream, a swirler device with twelve radial blades can be fitted.

The numerical simulation was made with the commercial solver FLUENT 6.0.12 for a Reynolds number:

$$\text{Re} = \frac{4(\dot{m}_{cb} + \dot{m}_{air})}{\pi\mu D} = 20520 \quad (35)$$

where $D=0.21\text{m}$ represents the furnace diameter, and μ is the viscosity of the oxidant. As previously presented, the turbulent flow was modeled by both RNG $K-\epsilon_K$ and the linear pressure strain RSM of Spalding (Fluent Inc. 1998), in addition to the two-layer approach of Wolfstein (Fluent Inc., 1998). In each case, this combination allowed us to integrate the equation system until the flow solid boundaries. The turbulent heat and mass fluxes were computed with the aid of algebraic relations $\alpha_t = \nu_t / \text{Pr}_t$, $D_t = \nu_t / \text{Sc}_t$, with $\text{Pr}_t=0.85$ and $\text{Sc}_t=0.7$. As a consequence, the volumetric turbulent parts of thermal and mass diffusion irreversibility components were modeled with the approximations (22) and (23).

For a correct computation of temperature and mass fraction gradients, the initial grid was twice refined within the domains defined by the reaction rate iso-values of $\omega=0.05 \text{ kmol/m}^3\cdot\text{s}$ and $\omega=0.5 \text{ kmol/m}^3\cdot\text{s}$. As a consequence, the final

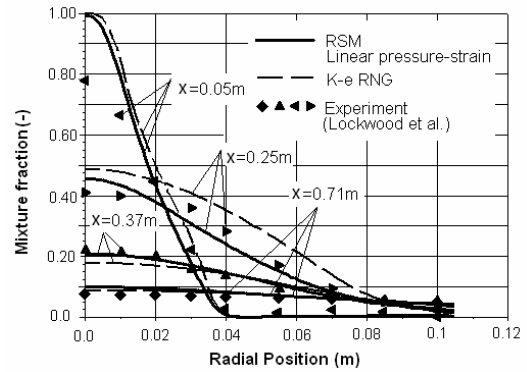


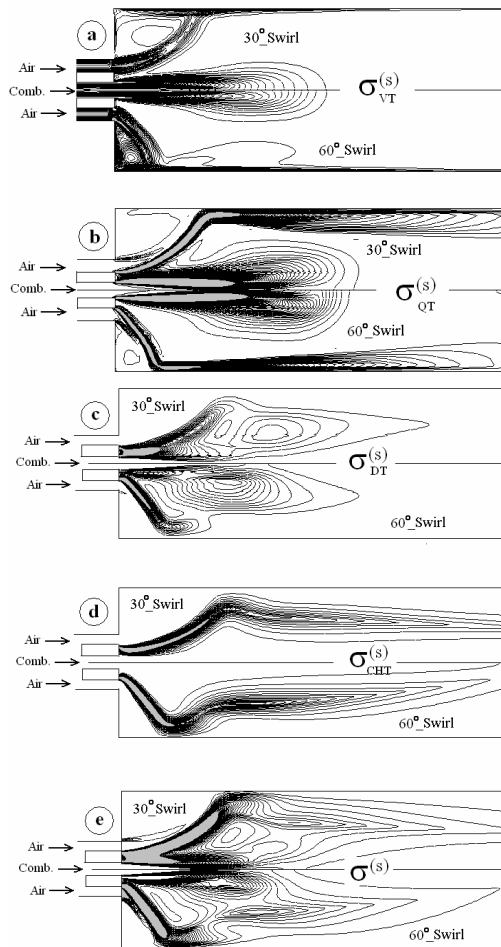
Figure 2. Radial profiles of mixture fraction for a swirl angle of air $\alpha=30^\circ$

unstructured grid of every numerical simulation was built from about 100,000 nodes.

Figure 2 presents the radial distributions of experimental and computed mixture fraction for a swirl angle of air stream, $\alpha=30^\circ$. As expected, on the first third of the inner jet length, both turbulence models fail to correctly predict the mixing near the flow axis. Anyway, the gap between the computed and the experimental values is quite unexpected and could be generated by the lower values of K simulated at the furnace inlets. But even in this region, starting from a radial position approximately equal with the radius of the fuel inlet section, the difference between the computed and experimental mixture fraction distributions quickly vanishes. Beginning from the second third of the inner jet, the accuracy of numerical prediction becomes acceptable and is continuously improving along the axis and in the radial direction. As a consequence, the length of the flame (defined as the axial distance measured from burner face at which the mixture fraction reach its stoichiometric value) is over predicted with only 1.5-2.5% by the two turbulence models. But concerning the mixture fraction distribution inside the reaction zone, clearly the RSM gives better results than $K-\epsilon_K$ RNG model. So, for all the irreversibility simulations presented here, only the linear pressure strain RSM turbulence closure model was retained.

Figures 3a-3d show the maps of the volumetric turbulent component of entropy generation rate. For the sake of clarity, the greatest and the smallest values of each irreversibility component were dropped, and the logarithmic scale was chosen for iso-value representation. Accordingly, the grey regions appearing in these distributions correspond to the dropped maximal values. It must be also emphasized that, for each component, the interval of iso-value representation was different.

All the volumetric turbulent components act in the flame sheet region where the chemical to



Figures 3. The distributions of volumetric turbulent irreversibility components and of the volumetric entropy generation rate for two values of swirl angle.

thermo-mechanical exergy conversion occurs. In this region, all the mean velocity, mean temperature and mean species mass fraction gradients have very high values. Through the mechanism of turbulent production, they extract an important part of the kinetic, thermal and mass diffusion exergy from the mean flow and transfer it to the larger eddies whose scales are comparable to the flow scale. This exergy, which is always accompanied by its corresponding energy, continuously relocates by the vortex-stretching mechanism to the smallest eddies where ε_K , ε_θ and ε_i dissipate it. As these processes are intensified, the turbulent components of volumetric irreversibility become greater. But, as revealed by Equation (27), the real benefit of interaction between the mean flow and the large eddies consists of the great enhancement of exergy transfer through its turbulent diffusion fluxes.

Another occurrence of turbulent irreversibility takes place in the region between the jet streams and the recirculation zone. Because of the gas inlet velocity, which is too high, the

penetration length of the inner stream into the recirculation zone is quite great. Clearly, it decreases as the swirl angle increases, but even for $\alpha=60^\circ$ it still remains important. Practically, on the penetration length, the recirculation flow region surrounds the gas stream. Then, the velocity, temperature and species mass fraction differences between these two regions generate the matching volumetric turbulent components, but they do not reach the corresponding values of those appearing in the flame sheet.

Figure 3e shows the distribution of whole volumetric irreversibility, computed as a sum of all its components. Obviously, in the flame sheet, the shape of volumetric irreversibility follows the distribution of both chemical and thermal turbulent components, while on the penetration length of the gas stream it pursues the spreading of diffusion and thermal ones.

Figures 3 also reveal the influence of swirl angle on the distributions of volumetric turbulent irreversibilities. The increment of α clearly moves the flame sheet in the upstream direction. As a consequence, the length of the irreversibility affected region decreases, while its width increases. Finally, the growth of the swirl angle until a certain value, depending on the burner geometry, increases the volume where the turbulent irreversibility is created, even if its axial distance diminishes.

Figures 4 present the variation of overall irreversibility components with the swirl angle. The numerical results show that all the overall mean components of the entropy generation rate are negligible compared to the corresponding turbulent ones. Their sum represents only 0.75-1.5% from the overall irreversibility of the reacting flow on the entire analyzed region. As revealed by Figure 4b, the turbulent viscous component can be also neglected because its contribution on the irreversibility field is less than 0.1%. The turbulent diffusion component, which is quite insensitive to the swirl angle variation, is responsible for only 10-12% from the whole exergy destruction.

The most important part of irreversibility is due to the chemical component, whose contribution at the overall rate of entropy generation is about 32-51% and to the turbulent thermal one, which represents 38-55% from the whole flow irreversibility. As a result, their sum is between 85-88%. This small gap of variation is caused by the change of the two components with respect to the swirl angle, which is totally different. As revealed by Figure 4b, while the turbulent thermal part of entropy generation increases with the rise of α , the chemical one decreases.

On the other hand, Figure 4b suggests the existence of an optimal swirl angle that mini-

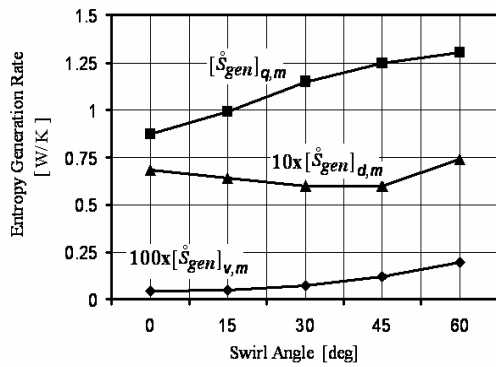


Figure 4a. Overall mean components variation with swirl angle

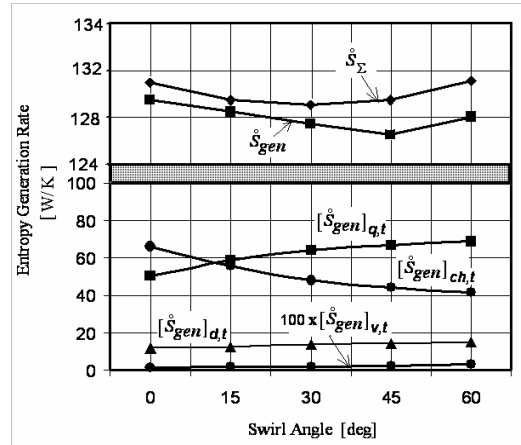


Figure 4b. Overall turbulent components and overall entropy flux variation with swirl angle

Figures 4. Entropy generation rate dependence with swirl angle

mizes the overall rate of entropy production. At lower values of α , the combustion occurs in a narrow sheet and the reaction products are post mixed outside this region with the rest of the air. In this case, the chemical irreversibility acts in a small volume, while the turbulent thermal irreversibility occurs in a greater one. When the swirl angle increases, the fuel is deflected to larger radii and mixes with a greater quantity of air. Beyond that, a fraction of heat which was previously transferred in the post mixing region is exchanged here, in the place where the chemical reaction takes place. Therefore, the occurrence volume of chemical reaction increases, while the volume in which the heat transfer takes place decreases. Clearly, the shapes of the chemical or turbulent thermal part of entropy production show that the overall irreversibility component slows down when its acting volume is increasing. For a certain value of α , the irreversibility affected regions become quite the same for every turbulent component. Now the turbulent irreversibility is spread in the greatest possible volume. Beyond this value of swirl angle, the characteristic volume of turbulent thermal and chemical irreversibilities diminishes because the radial spreading of fuel is blocked by the furnace walls. As a consequence, again the overall rate of entropy generation grows up. It follows that the spreading of turbulent irreversibilities as uniform as possible in an increased volume diminishes the exergy destruction. This conclusion confirms the equipartition principle of entropy production (Tondeur and Kvaalen, 1987).

Figure 3b also presents the variation of entropy convection flux (25) with the swirl angle. The bulk entropy balance Equation (24) is closed with an error between 1.3% for zero swirl and 2.75% for 60° swirl. Even the precision of closing decreases, the variation of entropy convec-

tion fluxes confirms the tendency of overall irreversibility variation with the swirl angle.

The irreversibility structure exposed by Figures 4 conflicts in a way with that revealed by the work of Dunbar and Lior (1994). Using the bulk level of exergy analysis and splitting the extent of chemical reaction into many steps, Dunbar and Lior (1994) computed the overall components of entropy production and found that the thermal one prevails while the chemical component, whose relative value strongly depends on the fuel type, always represents the second or the third irreversibility source of combustion processes. At the continuum level of second law analysis, the numerical simulation confirmed this irreversibility structure in the case of the laminar diffusion flames (Arpaci and Selamet, 1988, Datta, 2000, Stanciu et al., 2001). If it is accepted as a reference this irreversibility structure for the turbulent reacting flows, it must also be accepted that the fluctuating field affects in the same proportion all the entropy generation rate components. At this moment that is only a supposition. On the other hand, neglecting all momentum fluctuations of temperature and species mass fraction could affect the irreversibility structure revealed by the multi-species approach in a way that the turbulent chemical component is over predicted and the turbulent thermal one is under predicted in quite the same proportion. Figure 4b clearly proves that their sum is correctly quantified and the turbulence phenomena are entirely responsible for the overall rate of entropy generation in the diffusion flames.

Let us now discuss the implications of approximations (22)-(23) employed in the above numerical simulations. Clearly, in some regions of the flow, the volumetric turbulent parts of thermal and mass diffusion irreversibilities are under predicted, while in other ones are over

estimated. Of course not the whole exergy extracted from the mean flow and sent to the fluctuating field is always dissipated into heat at its extracting place. The difference is convected downstream by the mean velocity and is dissipated, but not entirely, in other flow regions. As a consequence, at the exit gate K , K_θ and K_i are greater than at the inlet ports, meaning that the same inequality holds for the fluctuating exergy too. But very often, the difference of fluctuating exergy between the outflow and inflow boundaries is quite small, so the relations (22)-(23) could represent acceptable approximations for the global rate calculus of entropy generation.

Conclusion

The goal of this work was to investigate the swirl angle influence on the turbulent diffusion flame irreversibilities. In accordance with the second law of thermodynamics, these irreversibilities were measured by the rate of entropy generation whose components are created by both the mean and the turbulent flow fields. The numerical simulations revealed that only the chemical turbulent thermal and turbulent diffusion components truly create the reacting flow irreversibilities. The contribution of the first two components of overall entropy production is about 85-88% and of the third lies between 10-12% from the whole reacting flow irreversibility. The rest, which is obviously negligible, belongs to the mean parts and to the turbulent viscous one. For minimizing exergy destruction, our mathematical and numerical models suggest that it is better to spread the reacting flow irreversibilities in a greater volume than concentrating them in a smaller region.

Following these conclusions we can propose two ways for reducing the combustion irreversibility by 1) adopting a flame stabilization technique, which reduces the turbulence levels of combustion, and 2) increasing the volume in which the exergy transfer processes take place, which means to reduce the thermal loading of the combustion chamber.

Nomenclature

A	Chemical affinity, J.kmol^{-1}
c_p	Specific heat at constant pressure, $\text{J.kg}^{-1}.\text{K}^{-1}$
D	Molecular mass diffusivity, $\text{m}^2.\text{s}^{-1}$
D_t	Turbulent mass diffusivity, $\text{m}^2.\text{s}^{-1}$
D_{im}	Diffusion coefficient of i -specie in gaseous mixture, $\text{m}^2.\text{s}^{-1}$
e_{h^*}	Specific exergy of total enthalpy, J.kg^{-1}
G	Free enthalpy, J.kmol^{-1}
h	Specific enthalpy, J.kg^{-1}

$J_\alpha^{(i)}$	Mass flux component in α direction, $\text{kgm}^{-2}.\text{s}^{-1}$
$J_\alpha^{(q)}$	Heat flux component in α direction, $\text{J.m}^{-2}.\text{s}^{-1}$
K	Turbulent kinetic energy, $\text{m}^2.\text{s}^{-2}$
K_θ	Fluctuating temperature variance, K^2
K_i	Fluctuating mass fraction variance of i -component
Le	Lewis number
M	Molar mass, kg.kmol^{-1}
N	Number of mixture's species
P	Pressure, Pa
Pr_t	Turbulent Prandtl number
R_i	Specific mass constant of ideal gas, $\text{J.kg}^{-1}.\text{K}^{-1}$
R_M	Universal constant of ideal gas, $\text{J.kmol}^{-1}.\text{K}^{-1}$
s	Specific entropy, $\text{J.kg}^{-1}.\text{K}^{-1}$
Sc_t	Turbulent Schmidt number
\dot{S}_{gen}	Overall entropy generation rate, W.K^{-1}
T	Thermodynamic temperature, K
u_α	Velocity component, m.s^{-1}
Y_i	Mass fraction of i -specie

Subscripts

0	Reference state
t	Turbulent
v,m	Viscous mean
v,t	Viscous turbulent
q,m	Thermal mean
q,t	Thermal turbulent
d,m	Diffusion mean
d,t	Diffusion turbulent
ch,t	Chemical turbulent

Greek symbols

α	Molecular thermal diffusivity, $\text{m}^2.\text{s}^{-1}$
	Swirl angle, deg
α_t	Turbulent thermal diffusivity, $\text{m}^2.\text{s}^{-1}$
$\delta_{\alpha\beta}$	Kronecker symbol
ε_K	Dissipation rate of turbulent kinetic energy, $\text{m}^2.\text{s}^{-3}$
ε_θ	Dissipation rate of mean fluctuating temperature variance, $\text{K}^2.\text{s}^{-1}$
ε_i	Dissipation rate of mean fluctuating mass fraction variance of i -component, s^{-1}
λ	Molecular thermal conductivity, $\text{W.m}^{-1}.\text{K}^{-1}$
λ_t	Turbulent thermal conductivity, $\text{W.m}^{-1}.\text{K}^{-1}$
ν	Molecular kinematic viscosity, $\text{m}^2.\text{s}^{-1}$
ν_t	Turbulent kinematic viscosity, $\text{m}^2.\text{s}^{-1}$

μ_i	Chemical potential of i -specie, J.kmol^{-1}
μ	Molecular viscosity, $\text{kg.m}^{-1}.\text{s}^{-1}$
μ_t	Turbulent viscosity, $\text{kg.m}^{-1}.\text{s}^{-1}$
$\sigma^{(s)}$	Volumetric rate of entropy generation, $\text{W.m}^{-3}.\text{K}^{-1}$
ζ_{ch}	Fraction of chemical molar exergy transferred to the thermomechanical exergy, J.kmol^{-1} .
ω	Rate of chemical reaction, $\text{kmol.m}^{-3}.\text{s}^{-1}$

Bibliography

- Abe, K., Kondoh, T., Nagano, Y., 1995: "A New Turbulence Model for Predicting Fluid Flow and Heat Transfer in Separating and Reattaching flows-II. Thermal Field Calculation", *Int. J. Heat Mass Transfer*, Vol. 38, No. 8, pp. 1467-1481.
- Arpaci, V., Selamet, A., 1988: "Entropy Production in Flames", *Combust. Flame*, 73 251-9.
- Bejan, A., 1983: *Entropy generation through fluid flow and heat transfer*, John Wiley & Sons.
- Borghi, R., 1988: "Turbulent Combustion Modelling", *Prog. Energy Combust. Sci.*, Vol. 14, pp. 245-292.
- Datta A., 2000: "Entropy Generation in a Confined Laminar Diffusion Flame", *Comb. Sci. Tech.*, Vol. 159, pp. 39-56.
- Dunbar, W. R., Lior, N., 1994: "Sources of Combustion Irreversibility" *Comb. Sci. Tech.*, Vol. 103, pp. 41-61.
- Deng, B., Wu, W., Xi, S., 2001: "A near two-equation heat transfer model for wall turbulent flows", *Int. J. Heat and Mass Transfer*, vol. 44, pp. 691-698.
- Ertesvag, I.S., Kolbu, J., 2005: "Entropy Production Modeling in CFD of Turbulent Combustion Flow", *Proceedings of ECOS 2005* pp. 265-272
- Fluent Inc., 1998: "User's Guide", *Fluent Incorporated*.
- Iandoli, C. L., Ertesvag, I.S., Sciubba, E., 2005 : "Using Entropy Production to Model Interaction between Combustion and Acoustics", *Proceedings of ECOS 2005*, pp 281-288.
- Magnusen, B. F., Hjertager, B. H., 1976: *On the Mathematical Model of Turbulent Combustion, with Special Emphasis on Soot Formation and Combustion*, 16th Symp. On Combustion.
- Libby, P.A., Williams, F.A., 1994 : *Turbulent Reacting Flows*, Academic Press, London.
- Lockwood, F.,C., El-Mahallawawy, F.,M., Spalding, D., B., 1974 : "An Experimental and Theoretical Investigation of Turbulent Mixing in a Cylindrical Furnace", *Combustion and Flame*, vol 23, pp. 283-293.
- Moran, J.M., Shapiro, N.H., 2006: *Fundamentals of Engineering Thermodynamics*, Fifth Edition, John Wiley&Sons.
- Sciubba, E., 1998: "Optimisation of Gas Turbine Components via Constrained Minimisation of the Local Entropy Production Rates", *Proceedings of NATO-ASI Workshop on Thermodynamics and Optimisation of Complex Energy Systems*, Constantza, Romania.
- Seki, Y., Kawamoto, N., Kawamura, H, 2003: "Proposal of Turbulent Heat Flux Model with Consideration of Linearity and its Application to Turbulent Channel Flow with Various Thermal Boundary Conditions", in *Turbulence, Heat and Mass Transfer 4*, Hanjalic et al. editors.
- Stanciu, D., Isvoranu, D., Marinescu, M., 2000: "Second Law Analysis of Turbulent Flat Plate Boundary Layer", *Int. J. of Applied Thermodynamics*, No. 3, pp. 99-104.
- Stanciu, D., Isvoranu, D., Marinescu, M., 2001: "Entropy generation rates diffusion flames", *Int. J. of Applied Thermodynamics*, No. 1, pp. 1-18.
- Stanciu, D., Marinescu, M., 2006: "Irreversibility Field in Turbulent Heat Convection Problems", *Oil & Gas Science and Technology*, Vol. 61, pp. 191-201.
- Sommer, T. P., So, R. M.C., Lai, Y. G., 1992: "A near-wall two-equation model for turbulent heat fluxes", *Int. J. Heat Mass Trans.*, Vol. 35, No. 12, pp. 3375-3387.
- Tondeur, D., Kvaalen, E., 1987: "Equipartition of entropy production: An optimal criterion for transfer and separation processes", *Eng. Chem. Res.*, Vol. 26, pp. 50-6